ANALYSIS OF STRONGLY NONLINEAR CIRCUITS WITH A FREQUENCY-DOMAIN METHOD COUPLED WITH A CONSISTENT LARGE–SIGNAL MODEL

Tapani Närhi

ESA-ESTEC
European Space Agency
PO Box 299, 2200 AG Noordwijk
The Netherlands

Abstract

The paper describes an analysis method that extends the applicability of frequency-domain methods to strongly nonlinear circuits. Nonlinearities are described with Chebyshev expansions which are evaluated with a numerically stable three-term recurrence formula. The method is coupled with a novel, measurement-based consistent modelling approach which allows improved accuracy in describing the frequency-dependence of the measured small-signal parameters. The analysis method and the modelling approach are verified by comparing measurements and calculations on a MESFET mixer, driven with two and three tones.

Introduction

Analysis of nonlinear microwave circuits using harmonic-balance (HB) methods is hampered by long computation time, when several excitation frequencies are present [1,2] and currently only three independent frequencies can be handled. Frequency-domain methods do not suffer from the same limitations: both the linear and nonlinear parts of the circuit are analysed in the frequency domain so that the time-consuming conversions between frequency and time domains are avoided. Also, the number of independent frequencies is not limited to three. The spectral-balance method of Rhyne et al. [3], which uses power series to approximate the nonlinear functions, is a well-known example of frequency-domain methods.

Modelling of nonlinear devices has been the weakest point of the frequency-domain approach. Nonlinear components are traditionally modelled in the time domain by using algebraic equations to describe the nonlinearities. Fitting power series into such equations is neither accurate nor elegant approach. In addition, strongly nonlinear functions require a large number of terms, e.g. several tens, in the series. High-degree terms typically have large coefficients and this degrades significantly the numerical accuracy. As a result, the application of the methods using power series has been limited to relatively weakly nonlinear circuits.

Frequency-domain method

This paper describes a frequency-domain method where both the limitations of the power series approach are removed: All the nonlinearities are represented with Chebyshev expansions instead of power series [4]. Excellent numerical stability of these expansions allows the use of high-degree terms without problems. A novel consistent modelling approach is presented, where the frequency-domain large-signal model is constructed directly from small-signal measurements through integration [5]. In comparison to other measurement-based models, e.g. [6], this approach makes possible more accurate representation of the frequency-dependence of the small-signal y-parameters of the device. Frequency-dependent characteristics (e.g. g_{ds}) are described in a natural way, in contrast to the HB methods, where the time-domain formulation of the nonlinearities makes it very difficult to construct a large-signal model that is accurate both at DC and RF. In fact, the earlier disadvantage of the frequency-domain approach, modelling of nonlinear devices, is now turned into an advantage.

Coupling the new large-signal model to the frequency-domain algorithm results in an effective and accurate method for analysing nonlinear circuits under multi-tone excitation. The large-signal model and the evaluation of the currents in the frequency domain are discussed in the following chapters.

Large-signal model

We assume that the currents at the two terminals of the intrinsic FET, driven with large-signal voltages $v_1(t)$, $v_2(t)$, can be written in the following form ($i = 1, 2$):

$$i_i(t) = g_i^{(0)}(v_1, v_2) + \\ + \dot{q}_i^{(1)}(v_1, v_2) + \ddot{q}_i^{(2)}(v_1, v_2) + \dddot{q}_i^{(3)}(v_1, v_2) + \cdots \quad (1)$$

where the dots indicate time-derivatives. This expression is an extension of the conventional quasi-static formulation [7,8], where only the first two terms of the series expansion are included, namely the static current through a nonlinear conductance, $g_i^{(0)}$, and the first order dynamic current through a nonlinear capacitance, $\dot{q}_i^{(1)}$. The higher order terms allow an accurate description of the frequency-dependence of the measured small-signal parameters, as will be shown below. We have a large-signal circuit model as shown in Figure 1.

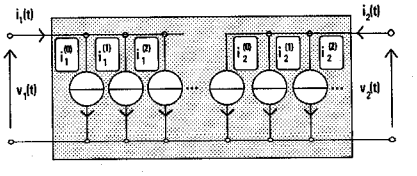

Figure 1 Large-signal circuit model for a nonlinear two-port.

CH3277-1/93/0000-0633$01.00 © 1993 IEEE

We require that the model is time-invariant, i.e., the nonlinear functions $g_i^{(0)}$ and $q_i^{(k)}$ are not explicit functions of time, but their time-dependence is solely through the dependence on the two controlling voltages. Further, we assume that the partial derivatives of these functions ($i, j = 1, 2, \quad k = 1, 2, \ldots$):

$$h_{ij}^{(0)}(v_1, v_2) = \frac{\partial g_i^{(0)}}{\partial v_j} \qquad h_{ij}^{(k)}(v_1, v_2) = \frac{\partial q_i^{(k)}}{\partial v_j} \tag{2}$$

depend only on the *instantaneous* voltages $v_1(t)$, $v_2(t)$, and not on their time-derivatives. With these assumptions, we can write the small-signal response of the device at port i, at DC bias point V_{10}, V_{20}, to a small variation in the voltages $dv_1(t)$, $dv_2(t)$ in the following form:

$$\begin{aligned} di_i(t) = {} & h_{i1}^{(0)}\, dv_1 + h_{i2}^{(0)}\, dv_2 + h_{i1}^{(1)}\, d\dot{v}_1 + h_{i2}^{(1)}\, d\dot{v}_2 + \\ & + h_{i1}^{(2)}\, d\ddot{v}_1 + h_{i2}^{(2)}\, d\ddot{v}_2 + \cdots \end{aligned} \tag{3}$$

Here all the partial derivatives are developed at the DC operating point. Moving to the frequency domain, we obtain the response to a small sinusoidal excitation $dv_1(f_k)$, $dv_2(f_k)$, at frequency f_k:

$$\begin{aligned} di_i(f_k) = {} & \left[h_{i1}^{(0)} + (j\omega_k) h_{i1}^{(1)} + (j\omega_k)^2 h_{i1}^{(2)} + \cdots \right] \cdot dv_1(f_k) + \\ & + \left[h_{i2}^{(0)} + (j\omega_k) h_{i2}^{(1)} + (j\omega_k)^2 h_{i2}^{(2)} + \cdots \right] \cdot dv_2(f_k) \end{aligned} \tag{4}$$

This can be compared with the measured small-signal response at a DC bias point (V_{10}, V_{20}):

$$\begin{aligned} di_i(f_k) = {} & y_{i1}(V_{10}, V_{20}, \omega_k) \cdot dv_1(f_k) + \\ & + y_{i2}(V_{10}, V_{20}, \omega_k) \cdot dv_2(f_k) \end{aligned} \tag{5}$$

Here $y_{ij}(V_{10}, V_{20}, \omega_k)$ are the measured small-signal y-parameters of the intrinsic FET at the bias point (V_{10}, V_{20}) and frequency f_k. We can now see that the higher order terms in (1) account for the frequency-dependence of the measured y-parameters: The second order term gives quadratic frequency-dependence to the real part of y_{ij}, the third order term causes cubic variation in the imaginary part of y_{ij} and so on. Thus we can identify each of the terms in Equation (3) directly from the measurements. The large-signal functions in (1) can then be calculated from the path-independent line integrals [6]:

$$\begin{aligned} g_i^{(0)}(v_1, v_2) = {} & I_{i0}(V_{10}, V_{20}) + \\ & + \int_{V_{10}}^{v_1(t)} h_{i1}^{(0)}(v_1, V_{20})\, dv_1 + \int_{V_{20}}^{v_2(t)} h_{i2}^{(0)}(v_1(t), v_2)\, dv_2 \end{aligned} \tag{6a}$$

$$q_i^{(k)}(v_1, v_2) = \int_{V_{10}}^{v_1(t)} h_{i1}^{(k)}(v_1, V_{20})\, dv_1 + \int_{V_{20}}^{v_2(t)} h_{i2}^{(k)}(v_1(t), v_2)\, dv_2 \tag{6b}$$

We can notice that it is important that the small-signal functions $h_{ij}^{(k)}$ do not depend on the time-derivatives of the voltages, since, if this were the case, it would be impossible to construct the large-signal functions $g_i^{(0)}$ and $q_i^{(k)}$ from static small-signal measurements only.

We observe that retaining only the first two terms in the series (1) shows resemblance to the Root model [6], where the frequency-dependence of the real parts of y_{11} and y_{12} (caused by the series connection of r_i with C_{gs} and r_{gd} with C_{gd}, respectively) are neglected. Keeping higher order terms in the series allows more accurate description of the frequency-dependence of the y-parameters of the intrinsic device in a consistent manner. The large-signal and small-signal models are inherently consistent, since the large-signal model is directly constructed from the small-signal characteristics through the line integrals (6). It should be noted that the 'delay-effect', corresponding to the imaginary part of y_{21} (which is normally described with τ in small-signal models) is represented in this model with $h_{21}^{(k)}$ (k odd) i.e., as a transcapacitance, as is done also in [6].

Next step in the modelling is finding the Chebyshev expansions to describe the dependence of each of the $h_{ij}^{(k)}$ functions on the two bias voltages. For example, for the static conductance we have:

$$h_{ij}^{(0)}(v_1, v_2) = \sum_{n=0}^{L} {\sum_{m=0}^{K}}' a_{mn} T_m(x) T_n(y) \tag{7}$$

Here x and y are the bias voltages, normalized to $[-1...+1]$ and K and L are the degrees of the expansion in the two dimensions. Standard surface-fitting procedures can be used to determine the Chebyshev coefficients a_{mn} [9]. The coefficients are then written into matrix $\mathbf{H}_{ij}^{(0)}$, which has the dimension (K+1) x (L+1). In practice, the coefficients are first determined for a high-degree expansion and the degree is then reduced as long as the approximation error is acceptable. With the Chebyshev expansions, in contrast to the power series, the coefficients of a lower-degree expansion are found simply by truncation of the higher degree coefficients at the desired point.

For the evaluation of the line integrals in (6), the Chebyshev coefficients for the integrated small-signal functions have to be determined. This is easily done from the coefficient matrices $\mathbf{H}_{ij}^{(k)}$ for the functions $h_{ij}^{(k)}$ by using the integration formula of the Chebyshev polynomials [10]. The resulting matrix of coefficients, integrated e.g. over x (that is, over v_1), is written as $\mathbf{H}_{ijx}^{(k)}$.

Evaluation of the currents in the frequency domain

The frequencies at which the circuit is to be analysed, are selected before solving the circuit equations. During the analysis, this set of frequencies, or the *frequency set*, is kept fixed and only those harmonics and intermodulation products falling on these frequencies are taken into account. The frequency set consists of P fundamental frequencies and their harmonics and intermodulation products. The total number of frequencies in the frequency set is N+1, including DC. In the frequency-domain methods, unlike in HB methods, P is not limited to three. The memory size and speed of the computer determine the maximum number of frequencies that can be handled. Each frequency can be written as: $\omega_k = k_1\omega_1 + k_2\omega_2 + \cdots + k_P\omega_P$. Maximum values for the

harmonic numbers $k_1, \ldots, k_P$ are selected so that all the significant frequencies are retained, but the total number of frequencies is kept to the minimum. In addition, the frequency set is limited by an independent parameter *maxIM*, which gives the maximum order of intermodulation products that are taken into account.

Evaluation of the nonlinear functions, expressed with Chebyshev expansions, requires multiplications between two waveforms. In the frequency domain the *convolution* of the two frequency spectra has to be calculated:

$$c(t) = a(t) \cdot b(t) \qquad \leftrightarrow \qquad \mathbf{c} = \mathbf{a} * \mathbf{b} \tag{8}$$

Here the asterisk stands for the convolution. All the waveforms are represented in the frequency domain with complex vectors of phasors and written with bold typeface. The convolution (8) is most conveniently calculated by multiplying the phasors of $\mathbf{a}$ with phasors of $\mathbf{b}$ (up to desired order) and using pre-calculated index vectors to assign the products to the corresponding frequencies in vector $\mathbf{c}$ [4]. Another way of calculating the convolution is from a matrix product [11]:

$$\underline{\mathbf{c}} = \mathbf{A} \cdot \underline{\mathbf{b}} \tag{9}$$

Here matrix $\mathbf{A}$ is obtained from vector $\mathbf{a}$ through a transformation, which consists of addition and assignment operations on the phasors of $\mathbf{a}$, with the help of pre-calculated index vectors [11]. Underlines in (9) indicate that $\mathbf{c}$ and $\mathbf{b}$ are represented with *real* vectors of dimension $(2N+1) \times 1$, instead of the normal complex representation of dimension $(N+1) \times 1$. This formulation is used when a time-domain *division* $b(t) = c(t) / a(t)$ has to be calculated in the frequency domain. From (9) we can see that in this case the unknown vector $\mathbf{b}$ is obtained from the solution of a set of linear equations:

$$\underline{\mathbf{b}} = \mathbf{A}^{-1} \cdot \underline{\mathbf{c}} \tag{10}$$

The same principle is used in constructing the Jacobian [12].

Functions approximated with Chebyshev expansion are evaluated in a numerically stable manner by using the well-known Clenshaw's recurrence formula [10]. In the frequency domain, a two-dimensional function $f(x,y)$ is evaluated from the following recursion, by first calculating vectors $\mathbf{c}_i$ in y-direction for each $i = K, K-1, \ldots, 0$:

$$\begin{aligned} &\mathbf{b}_{L+2}^{(i)} = \mathbf{b}_{L+1}^{(i)} = \mathbf{0} \\ &\mathbf{b}_j^{(i)} = 2 \cdot \mathbf{y} * \mathbf{b}_{j+1}^{(i)} - \mathbf{b}_{j+2}^{(i)} + a_{ij}\boldsymbol{\delta} \qquad j = L, L-1, \ldots, 0 \\ &\mathbf{c}_i = \tfrac{1}{2}\left(\mathbf{b}_0^{(i)} - \mathbf{b}_2^{(i)}\right) \end{aligned} \tag{11a}$$

Next, these coefficient vectors are used to evaluate the function in x-direction:

$$\begin{aligned} &\mathbf{d}_{K+2} = \mathbf{d}_{K+1} = \mathbf{0} \\ &\mathbf{d}_i = 2 \cdot \mathbf{x} * \mathbf{d}_{i+1} - \mathbf{d}_{i+2} + \mathbf{c}_i \qquad i = K, K-1, \ldots, 0 \\ &\mathbf{f}(\mathbf{x},\mathbf{y}) = \tfrac{1}{2}\left(\mathbf{d}_0 - \mathbf{d}_2\right) \end{aligned} \tag{11b}$$

Here $\mathbf{x}$ and $\mathbf{y}$ are the normalized voltages $\mathbf{v}_1$ and $\mathbf{v}_2$, matrix $\mathbf{A}$ contains the Chebyshev coefficients a_{ij} with dimension $(K+1) \times (L+1)$ and $\boldsymbol{\delta}$ is a $(N+1) \times 1$ vector, with the first element equal to one and the others are zeros. We use a short notation with operator T{} for this recursion:

$$\mathbf{f}(\mathbf{x},\mathbf{y}) = \mathrm{T}\{\mathbf{A}, \mathbf{x}, \mathbf{y}\} \tag{12}$$

We are now able to calculate the large-signal functions, given in Equation (6), directly in the frequency domain, for given spectra of the driving voltages:

$$\begin{aligned} \mathbf{g}_i(\mathbf{v}_1,\mathbf{v}_2) = {} & \mathrm{T}\{\mathbf{D}_i^{DC}, x_0, y_0\}\,\boldsymbol{\delta} + \\ & + \alpha \cdot \left[\, \mathrm{T}\{\mathbf{H}_{i1x}^{(0)}, \mathbf{x}, y_0\boldsymbol{\delta}\} - \mathrm{T}\{\mathbf{H}_{i1x}^{(0)}, x_0\boldsymbol{\delta}, y_0\boldsymbol{\delta}\} \,\right] + \\ & + \beta \cdot \left[\, \mathrm{T}\{\mathbf{H}_{i2y}^{(0)}, \mathbf{x}, \mathbf{y}\} - \mathrm{T}\{\mathbf{H}_{i2y}^{(0)}, \mathbf{x}, y_0\boldsymbol{\delta}\} \,\right] \end{aligned} \tag{13a}$$

$$\begin{aligned} \mathbf{q}_i^{(k)}(\mathbf{v}_1,\mathbf{v}_2) = {} & \alpha \cdot \left[\, \mathrm{T}\{\mathbf{H}_{i1x}^{(k)}, \mathbf{x}, y_0\boldsymbol{\delta}\} - \mathrm{T}\{\mathbf{H}_{i1x}^{(k)}, x_0\boldsymbol{\delta}, y_0\boldsymbol{\delta}\} \,\right] + \\ & + \beta \cdot \left[\, \mathrm{T}\{\mathbf{H}_{i2y}^{(k)}, \mathbf{x}, \mathbf{y}\} - \mathrm{T}\{\mathbf{H}_{i2y}^{(k)}, \mathbf{x}, y_0\boldsymbol{\delta}\} \,\right] \end{aligned} \tag{13b}$$

Here x_0, y_0 is the normalized DC operating point, $\mathbf{D}_i^{DC}$ is the matrix of Chebyshev coefficients for the DC current in port i and α and β account for the change of variables in the calculation of the line integrals:

$$\alpha = \frac{dv_1}{dx} = \frac{V_{1\max} - V_{1\min}}{2} \qquad \beta = \frac{dv_2}{dy} = \frac{V_{2\max} - V_{2\min}}{2} \tag{14}$$

The current at port i of the device, given in Equation (1), is then calculated in the frequency domain:

$$\begin{aligned} \mathbf{i}_i(\mathbf{v}_1,\mathbf{v}_2) = {} & \mathbf{g}_i(\mathbf{v}_1,\mathbf{v}_2) + \\ & + \boldsymbol{\Omega} \cdot \mathbf{q}_i^{(1)}(\mathbf{v}_1,\mathbf{v}_2) + \boldsymbol{\Omega}^2 \cdot \mathbf{q}_i^{(2)}(\mathbf{v}_1,\mathbf{v}_2) + \cdots \end{aligned} \tag{15}$$

Here $\boldsymbol{\Omega}$ is a $(N+1) \times (N+1)$ matrix with the angular frequencies $j\omega_k$ in the diagonal and zero elsewhere.

Measured and calculated results

A large-signal model was constructed for a 1 x 300 mm monolithic MESFET ($V_T = -1.5$ V) using the principle described above. First, DC measurements were made and then s-parameters were measured (on wafer) over the entire operating range of bias voltages (161 bias points, $V_{gs} = -3 \ldots 0.75$ V, $V_{ds} = 0 \ldots 5$ V) and frequencies (0.1...18.1 GHz). Parasitics were extracted with the help of the measurements on cold FET and Chebyshev expansions were fitted on the y-parameters of the intrinsic FET.

Next, mixer measurements were made on wafer, using the same FET chip, with both the drain and source terminated to 50 Ω. The effect of the bias voltages and local oscillator (LO) power on the conversion gain ($f_{RF} = 0.8$ GHz, $f_{LO} = 0.9$ GHz) were measured around the experimentally found best operating point $V_{gs} = -1.3$ V, $P_{LO} = 6$ dBm at drain voltage $V_{ds} = 2.5$ V. These measurements were simulated with the frequency-domain algorithm with three harmonics of RF, five harmonics of LO and intermodulation (IM) products up to order five taken into account, or with 27 frequencies in total. Figures 2 and 3 show both the measured and simulated results. We can see that the effects of bias voltages and LO power are accurately predicted by the simulation.

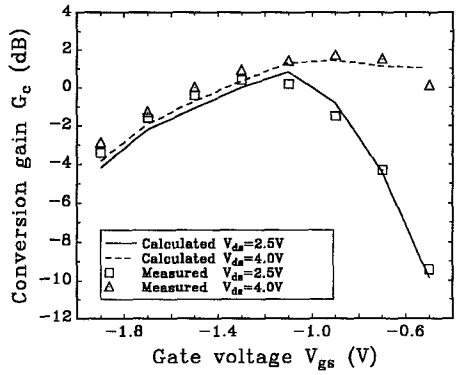

Figure 2 Measured (symbols) and calculated (lines) conversion gain versus gate bias.

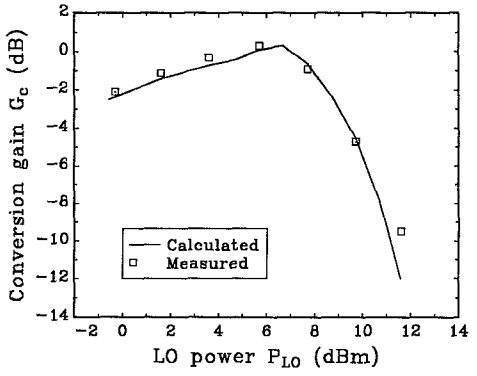

Figure 3 Measured (symbols) and calculated (lines) conversion gain versus local oscillator power.

Finally, mixer intermodulation measurements were made at the same operating point by sweeping the power level of two closely (5 MHz) separated RF tones and observing the power levels of the IF and third order intermodulation products on a spectrum analyzer. Again, the measurement was simulated using the frequency-domain method. Three harmonics of the two RF signals, five harmonics of the LO and intermodulation products up to order five, or 104 frequencies in total, were taken into account. In order to be able to extend the simulation to relatively high power levels, i.e., past saturation of the IF, it was necessary to widen the normalization range of the gate voltage to −5...0.8 V by extrapolation. Measured and simulated results are shown in Figure 4, and again we can notice excellent agreement. The computer used in all the calculations was a 486 machine with 8 Mbyte RAM.

Conclusions

An analysis method has been presented that extends the applicability of frequency-domain methods to strongly nonlinear circuits. A novel frequency-domain modelling scheme for nonlinear devices has been developed. The model is inherently self-consistent due to the measurement-based construction: The large-signal currents are directly constructed from small-signal y - parameters through integration. The model has the advantage that the frequency-

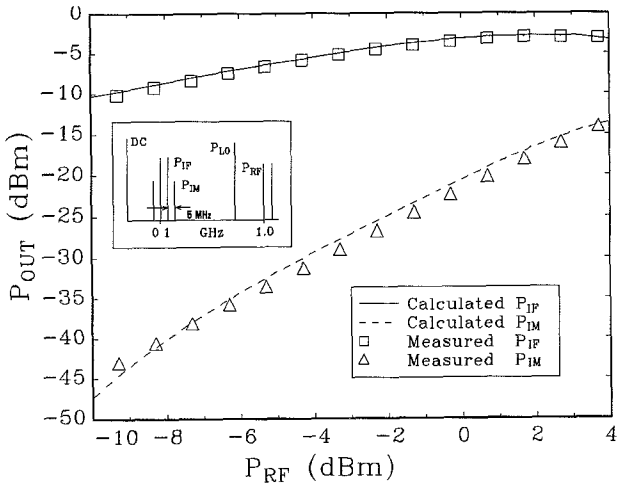

Figure 4 Measured (symbols) and calculated (lines) IF and IM levels at the output of the mixer.

dependence of the measured small-signal parameters can be described as accurately as desired. The model consists of polynomials, therefore, all the derivatives of interest exist and are continuous. Frequency-domain construction guarantees inherent accuracy in describing frequency-dependent characteristics, like g_{ds}, of the nonlinear devices.

The analysis method and modelling approach have been experimentally verified by comparing measured and simulated results on a monolithic MESFET operating as mixer. The efficiency of the frequency-domain method has been demonstrated by analysing the intermodulation distortion of the mixer with three independent tones and over 100 frequencies in total, driven past saturation with strong RF signals, on a personal computer.

Acknowledgment

This work was partly done during my stay at the Telecommunications Laboratory of VTT (Finland).

References

[1] S.A. Maas and D.A. Neilson, "Modeling MESFET's for intermodulation analysis of mixers and amplifiers," *IEEE Trans Microwave Theory Techn*, vol MTT-38, no. 12, pp 1964-1971, Dec 1990

[2] V. Rizzoli, C. Cecchetti, A. Lipparini, F. Mastri, "General-purpose harmonic balance analysis of nonlinear microwave circuits under multitone excitation," *IEEE Trans Microwave Theory Techn*, vol. MTT-36, pp 1650-1659, Dec. 1988.

[3] G.W Rhyne, M B Steer and B.D. Bates, "Frequency-domain nonlinear circuit analysis using generalized power series," *IEEE Trans Microwave Theory Techn.*, vol. MTT-36, no. 2, pp 379-387, Febr 1988

[4] T. Narhi, "Multi-frequency analysis of nonlinear circuits using one- and two-dimensional series expansions," in *Proc. 19th European Microwave Conf*, Sept 1989, pp. 375-379, 1989

[5] T. Närhi, "Black-box modelling of nonlinear devices for frequency-domain analysis," *in Proc. 22h European Microwave Conf.*, Aug 1992, pp. 1109-1114, 1992

[6] D.E Root, S. Fan and J. Meyer, "Technology independent large-signal non quasi-static FET models by direct construction from automatically characterized device data," in *Proc 21st European Microwave Conf.*, Sept. 1991, pp. 927-932, 1991.

[7] K S. Kundert and A. Sangiovanni-Vincentelli, "Simulation of nonlinear circuits in the frequency domain," *IEEE Trans. Computer-Aided Design*, vol CAD-5, pp 521-535, Oct. 1986.

[8] D.E. Root, S. Fan and J. Meyer, "Technology-independent large-signal FET models: A measurement based approach to active device modelling," in *Proc. 15th ARMMS Conf*, Sept. 1991

[9] C.W Clenshaw and J.G. Hayes, "Curve and surface fitting," *J. Inst. Maths. Applics*, vol 1, pp.164-183, 1965

[10] L Fox and I.B. Parker, *Chebyshev polynomials in numerical analysis*, Oxford University Press, 1968

[11] T. Närhi, "Frequency domain modelling of strongly nonlinear components," in *Proc. 3rd Asia-Pacific Microwave Conf.*, pp 325-328, Tokyo, September 18-21, 1990.

[12] T. Närhi, to be published